Journal of Energy Chemistry 25 (2016) 832–839

Contents lists available at ScienceDirect

Journal of Energy Chemistry

journal homepage: www.elsevier.com/locate/jechem

http://www.journals.elsevier.com/journal-of-energy-chemistry/

Improved hydrogen storage properties of MgH_2 catalyzed with K_2NiF_6 ☆

N. N. Sulaiman, N. Juahir, N. S. Mustafa, F. A. Halim Yap, M. Ismail*

School of Ocean Engineering, Universiti Malaysia Terengganu, 21030 Kuala Terengganu, Malaysia

ARTICLE INFO

Article history:
Received 3 February 2016
Revised 22 March 2016
Accepted 28 March 2016
Available online 29 April 2016

Keywords:
Hydrogen storage
Solid state storage
Magnesium hydride
Catalyst

ABSTRACT

In this study, the hydrogen storage properties of MgH_2-X wt% K_2NiF_6 ($X = 5$, 10, 15, 20, and 50) were investigated for the first time. From the analysis of the onset desorption temperature and isothermal de/absorption kinetics, it was shown that $MgH_2 + 5$ wt% K_2NiF_6 sample has the best performance. The 5 wt% doped sample started to release hydrogen at about 260 °C, which was a reduction of about 95 °C and 157 °C compared with the as-milled and as-received MgH_2. In addition, the de/absorption kinetics of the $MgH_2 + 5$ wt% K_2NiF_6 were also improved significantly compared to the un-doped MgH_2. The apparent activation energy for hydrogen desorption exhibited the decrement from 167.0 kJ/mol for as-milled MgH_2 to 111.0 kJ/mol with the addition of 5 wt% K_2NiF_6. Moreover, the X-ray diffraction spectra displayed the formation of new phases of KF, KH, Mg_2Ni and Mg_2NiH_4 by doping the K_2NiF_6 with MgH_2 after the dehydrogenation and rehydrogenation processes. The scanning electron microscope results revealed that MgH_2 doped with 5 wt% K_2NiF_6 demonstrated the smallest particle size compared to the as-received and as-milled MgH_2. It is believed that the formation of in situ active species of KF, KH, and Mg_2Ni could provide a synergetic catalytic effect in enhancing the hydrogen sorption properties of MgH_2.

1. Introduction

Hydrogen is one of the ideal environmental friendly energy carriers because the products from its combustion are only water and water vapors, which are non-toxic components. Furthermore, hydrogen can be considered as the best choice for fuel in the future, such as in automotive applications. However, U.S. DOE's 2017 goal [1] stated that large volumetric (≥ 40 g/L) and gravimetric (5.5 wt%) densities are needed for on-board hydrogen storage in fuel cell based vehicles. Thus, an alternative method in finding a promising method to store hydrogen is needed to fulfill the DOE's target. Currently, there are three possible approaches to store hydrogen, namely compressed hydrogen gas, cryogenic hydrogen, and solid-state hydrogen storages. Compared to high-pressure and cryogenic liquid, solid-state storage has become a promising option due to its advantages, such as high gravimetric hydrogen capacity, safety, and space for storage.

Among the solid-state hydrogen storage materials, MgH_2 could be perceived as one of the most efficient materials that has excellent potential for automotive applications due to its high hydrogen storage capacity of up to 7.6 wt%, superior reversibility and low cost [2]. Nevertheless, the application of MgH_2 is limited by the high decomposition temperature with slow de/absorption kinetics and too thermodynamically stable (76.0 kJ/mol H_2) [3]. The high temperature is not suitable for practical on-board applications. Thus, to overcome these disadvantages, many studies have been done to improve the thermodynamics and kinetics properties by reducing the grain size [4–6], doping with catalyst [7,8], and using destabilizing concept (reacting with other metal hydrides) [9–13]. Among the three efforts, doping MgH_2 with catalyst by ball milling method has been the focus of intensive research because it has shown a significant effect on the hydrogen storage properties of MgH_2. Catalysis doping that has been widely studied on MgH_2 through mechanical milling to cope with the kinetic limitations is transition metals [14], hydrogen storage alloys [15–17], metal halide [18–23], metal oxides [24–27], and carbon based catalyst [28].

Among the various catalysts, the highly effective type has been shown by the transition-metal compounds resulting from the high affinity of the transition-metal cations towards hydrogen [19,29–33]. To the best of the author's knowledge, Ni is one of the most promising catalyst that can improve the performance of hydrogenation properties of MgH_2. Based on a study

☆ This work was supported by Ministry of Higher Education Malaysia Fundamental Research Grant Scheme (FRGS 59362).

* Corresponding author. Tel: +609 6683487; Fax: +609 6683991.
E-mail address: mohammadismail@umt.edu.my (M. Ismail).

http://dx.doi.org/10.1016/j.jechem.2016.04.015

conducted on transition metal by Liang et al. [14], it was found that the de/rehydrogenation kinetics of MgH_2 were enhanced by adding 5 wt% transition metal (Ti, V, Mn, Fe, Ni) compared to un-doped MgH_2. Additionally, Zhang et al. [34] reported that by doping MgH_2 with Ti and Ni, the hydrogen desorption enthalpy and initial dehydrogenation temperature of MgH_2 were improved significantly. Between the two materials, the doping effect of Ni is highly notable. Moreover, a study on the effect of Ni, $LiBH_4$, and LiH on the MgH_2 in terms of the hydrogen absorption/desorption properties demonstrated that Ni-doped MgH_2 could achieve the best hydrogen absorption/desorption kinetics via short-time milling [35]. On the other hand, Mao et al. [3] reported that Ni is one of the best catalysts to enhance the sorption kinetics of Mg-based materials and to decrease the dehydrogenation temperature. Ni is a good catalyst in helping the dissociation process of hydrogen molecules and the recombination of hydrogen atoms toward the molecular state. Thus, the Mg–H bond could be activated by the catalyst when the hydrogen desorption takes place.

But, further enhancements are still sensible to be carried out. Therefore, it is of interest to further investigate the addition of Ni with other materials as a catalyst for MgH_2 that can enhance its hydrogen storage properties and concurrently develop greater understanding on the modification of MgH_2 for solid-state hydrogen storage. Thus, adding Ni with F-containing catalytic species is one of the way to enhance the hydrogen storage properties of MgH_2. Luo et al. [36] found that $MgH_2 + 2$ mol% NbF_5 could absorb 5 wt% hydrogen in 12 s and desorb 4.4 wt% in 5 h. It was revealed that the kinetic improvement of MgH_2 was influenced by both metal and fluorine anions. Meanwhile, the catalytic effect of the F anion was also proved in a study conducted by Ma et al. [20,37]. TiF_3 exhibits the best catalytic effect on the hydrogen sorption kinetics enhancement of MgH_2 over $TiCl_3$. Similar results had been reported by Yin et al. [38], which indicated that F actively played the catalytic role in the improvement of $NaAlH_4$–TiF_3 system. In the meantime, Deledda et al. [39] studied the role of fluorine in MgH_2 using 5 mol% FeF_3 and 5 mol% NiF_2 that are doped with MgH_2. The results obtained shown that the onset desorption temperature has been reduced dramatically.

Furthermore, potassium (K) also can be considered as a best candidate for a catalyst to combine with Ni and F-containing catalytic species to enhance the hydrogen storage properties of MgH_2. For an example, K affected the $NaAlH_4$ in enhancing the dehydrogenation properties [40]. On the other hand, Wang et al. [41] reported that hydrogen desorption properties in $Mg(NH_2)_2$/2LiH had been improved by adding with potassium, by increasing the rates of the reactions and lower down the overall reaction temperature. Dong et al. [42] studied the catalytic effects of several kinds of potassium compounds to enhance the kinetics properties of the hydrogen desorption reaction in LiH–NH_3 system. The study reported that the additives of potassium compound shown that the catalytic effect improves the reaction, which are larger than as-milled LiH.

Therefore, it is quite attractive to mix these three elements together, including K, Ni and F as catalysts to enhance the hydrogen storage properties of MgH_2. To date and to our knowledge, no studies had reported the effects of K_2NiF_6 on the hydrogenation performance of MgH_2 for solid-state hydrogen storage. In this paper, we propose to investigate the different amounts of K_2NiF_6 in the hydrogen storage properties of MgH_2. The samples were ball milled together to prepare the mixtures of MgH_2/K_2NiF_6. The hydrogen storage properties and reaction mechanisms of the samples were investigated using Sieverts-type pressure-composition-temperature (PCT) apparatus, X-ray diffraction (XRD) and scanning electron microscope (SEM). Additionally, the possible catalytic mechanism is also discussed in this paper.

2. Experimental

Pure MgH_2 (hydrogen storage grade, 98% purity) and K_2NiF_6 (99% purity) were purchased from Sigma Aldrich, where both materials were used without any modification. All the samples handling, including weighing and loading were performed in an MBraun Unilab glove box filled with high-purity argon atmosphere to eliminate the influences of oxygen and water moisture. Thereafter, the MgH_2 and K_2NiF_6 were loaded into a sealed stainless steel vial together with four hardened stainless steel balls. The ratio of the weight of the balls to the weight of the powder is 40:1. The samples were then milled for 1 h in a planetary ball mill (NQM-0.4), where the processes are 15 min of milling, 2 min of rest, and repeated for another 2 cycles in different directions at the rate of 400 rpm. The pure MgH_2 was also prepared under the same conditions for fair comparison on the catalytic effects.

Sievert-type pressure–composition–temperature (PCT) apparatus (Advanced Materials Corporation) or also known as gas reaction controller (GRC) was used for the temperature-programmed-desorption (TPD) and de/rehydrogenation experiments. About 100 mg of the sample was loaded into a sample vessel in the glove box. For the TPD experiments, all the samples were heated in a vacuum chamber from room temperature to 450 °C, with an incremental heating rate of 5 °C/min. The lowest decomposition temperature of the samples was determined by measuring the amount of desorbed hydrogen. Meanwhile, the de/rehydrogenation kinetics experiments were conducted at the desired temperature with initial hydrogen pressures of 1.0 atm and 33.0 atm.

Differential scanning calorimetry (DSC) analysis of the as-prepared powder samples was carried out using a Mettler Toledo TGA/DSC 1. About 2–6 mg of the sample was loaded into an alumina crucible in the glove box. Subsequently, the crucible was placed in a sealed glass bottle in order to prevent oxidation during the transfer from the glove box to the DSC apparatus. An empty alumina crucible was used for reference. The samples were heated from room temperature to 500 °C under Ar atmosphere, and the heating rate was 30 °C/min.

The phase structures of the samples after milling, desorption, and absorption were performed by using a Rigaku MiniFlex X-ray diffractometer with Cu $K\alpha$ radiation. Scans in the range of θ–2θ were carried out over diffraction angles from 20° to 80° with a speed of 2.00°/min. To minimize the oxidation of the sample, a small amount of sample was spread uniformly on the sample holder and covered with scotch tape and followed by sealing with plastic wrap. Meanwhile, scanning electron microscope (SEM; JEOL JSM-6360LA) was used to investigate the surface morphology of the samples by preparing the samples on carbon tape and then coating it with gold spray under vacuumed condition. The samples were also prepared in the glove box in order to minimize the oxidation.

3. Results and discussion

3.1. Dehydrogenation temperature

Fig. 1 presents the temperature-programmed-desorption (TPD) curves for the dehydrogenation of as-received MgH_2, as-milled MgH_2, and the MgH_2 doped with different ratios of K_2NiF_6, namely 5 wt%, 10 wt%, 15 wt%, 20 wt%, and 50 wt%. From the TPD results, it was proven that increasing the catalyst ratio from 5 wt% to 50 wt% demonstrated a reduction of the onset desorption temperature compared to the un-doped MgH_2. The as-received MgH_2 started to

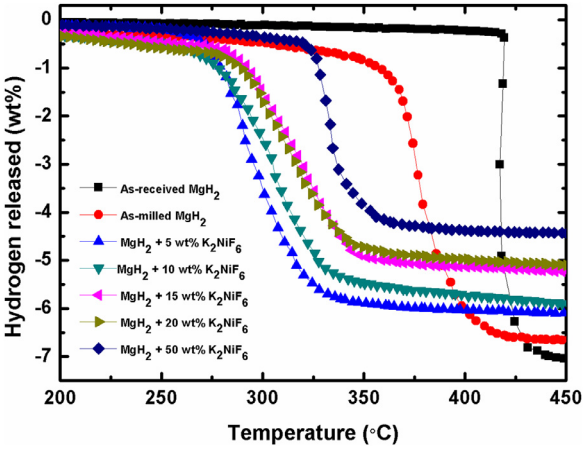

Fig. 1. TPD curves for the dehydrogenation of as-received MgH_2, as-milled MgH_2 and the MgH_2 doped with 5 wt%, 10 wt%, 15 wt%, 20 wt%, and 50 wt% K_2NiF_6.

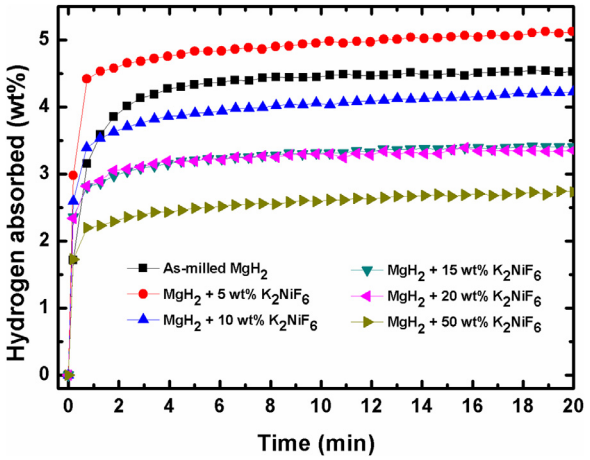

Fig. 2. Isothermal rehydrogenation kinetics curves of as-milled MgH_2 and the MgH_2 doped with 5 wt%, 10 wt%, 15 wt%, 20 wt% and 50 wt% K_2NiF_6 at 320 °C and under 33.0 atm.

release hydrogen at about 417 °C, with a total dehydrogenation capacity of 7.1 wt% H_2 at 450 °C. Meanwhile, after milling, the onset desorption temperature of MgH_2 slightly dropped to about 355 °C with total hydrogen desorption of 6.7 wt%. This results showed that the milling process also affected the onset desorption temperature of MgH_2, due to the larger surface area in magnesium surfaces. It means that after ball milled, the size of particles become smaller and larger specific surface area was achieved, resulting in decrement of hydrogen diffusion length. Based on the graph, there was a decrement in the hydrogen desorption capacity of the MgH_2 after milling. The decrement could happen due to the hydrogen released by MgH_2 during the milling process. As a result, the un-milled MgH_2 showed higher capacity compared to the milled MgH_2.

After doping with K_2NiF_6, the onset desorption temperature of the MgH_2 greatly improved. All the samples doped with different ratios of K_2NiF_6 started to release hydrogen below 330 °C. The 5 wt% doped sample started to decomposed at about 260 °C, which decreased about 95 °C compared to the as-milled MgH_2 with a total dehydrogenation capacity of 6.1 wt% H_2. For the MgH_2 that doped with 10 wt% K_2NiF_6, the dehydrogenation temperatures reduced to about 270 °C, which is a 85 °C reduction in the desorption onset temperature of MgH_2 and the amount of hydrogen released was decreased to about 5.9 wt%. Further increasing the amount of doping to 15 wt% and 20 wt% decreased the onset desorption temperature to about 275 °C and 280 °C, however, the amount of hydrogen desorption capacity slightly decreased to about 5.3 wt% and 5.1 wt% H_2, respectively. Meanwhile, MgH_2 doped with 50 wt% was also studied on the patterns of the onset desorption temperature to support the results obtained. From the results, it is still proven that adding a big amount of catalyst also enhances the decomposition temperature by releasing hydrogen at the temperature of 320 °C and reduces the amount of hydrogen released at only about 4.4 wt%. A same condition was found by Ismail [21] for $FeCl_3$-doped MgH_2, in which the decrement of the hydrogen released in the higher doping amounts may be due to the addition of relatively high levels of catalyst that led to the excessive catalytic effects. Ranjbar et al. [43] also claimed that the diffusion paths have been blocked due to the limitations of the hydrogen diffusion that caused excessive doping of samples. All these results suggest that K_2NiF_6 that acted as the catalyst to the MgH_2 could play a catalytic role, and thus improve the onset desorption temperature of MgH_2.

3.2. Re/dehydrogenation kinetics

In order to investigate the reversibility of the MgH_2 doped with 5 wt%, 10 wt%, 15 wt%, 20 wt% and 50 wt% K_2NiF_6, the rehydrogenation of the dehydrogenated sample was carried out under 33.0 atm of H_2 and at 320 °C. Additionally, the un-doped MgH_2 was also examined for comparison. Fig. 2 compares the isothermal rehydrogenation kinetics of the as-milled MgH_2 and the MgH_2 doped with different ratios of K_2NiF_6, namely 5 wt%, 10 wt%, 15 wt%, 20 wt% and 50 wt%. From the graph, it can be seen that the doped composite of 5 wt% has the fastest kinetics rate. In addition, the sample shows better hydrogen absorption properties than the un-doped composite. A hydrogen absorption capacity of 4.6 wt% was reached after 2 min in the MgH_2+5 wt% K_2NiF_6. While the as-milled MgH_2 only absorbed 3.9 wt% of hydrogen and required about 20 min to achieve the same capacity with the MgH_2+5 wt% K_2NiF_6. From the results, it can be seen that the addition of small amount of additive could enhance both the absorption and desorption kinetics of MgH_2. The results is in good agreement with the previous study conducted by Webb [44], in which the absorption and desorption reaction kinetics could be improved by the addition of small amounts of the additives, which is between 1 and 5 mol%. On the other hand, for the 10 wt%, 15 wt%, 20 wt% and 50 wt% doped MgH_2, it is revealed that the hydrogen absorption capacities are 3.7 wt%, 3.0 wt%, 3.1 wt% and 2.3 wt%, respectively, within 2 min.

Fig. 3 shows the comparison of the dehydrogenation kinetics between the as-milled MgH_2 and MgH_2 doped with 5 wt%, 10 wt%, 15 wt%, 20 wt% and 50 wt% K_2NiF_6, where both were conducted under 1.0 atm pressure at a temperature of 320 °C. As shown in the graph, the doped samples displayed a remarkable improvement compared to the un-doped MgH_2. The MgH_2 doped with 5 wt%, 10 wt%, 15 wt%, 20 wt% and 50 wt% K_2NiF_6 released about 4.9 wt%, 3.9 wt%, 3.8 wt%, 3.2 wt% and 1.8 wt% hydrogen within 10 min, respectively. Meanwhile, it can be seen that almost no hydrogen was released at this temperature from the as-milled MgH_2 sample within the same period of time. From the analysis above, K_2NiF_6 also could be concluded as a good catalyst in improving the desorption kinetics.

The results of the onset desorption temperature and isothermal de/absorption kinetics have clearly shown that MgH_2+5 wt% K_2NiF_6 exhibits the best performance among the ratios in enhancing the hydrogen storage properties of MgH_2. Therefore, 5 wt% doping amount can be considered as the best sample to combine

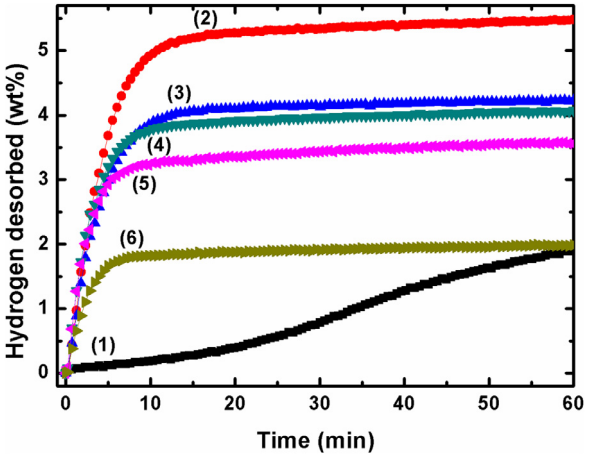

Fig. 3. Isothermal deydrogenation kinetics curves for (1) as-milled MgH_2 and MgH_2 doped with (2) 5 wt%, (3) 10 wt%, (4) 15 wt%, (5) 20 wt% and (6) 50 wt% K_2NiF_6 at 320 °C and under 1.0 atm hydrogen pressure.

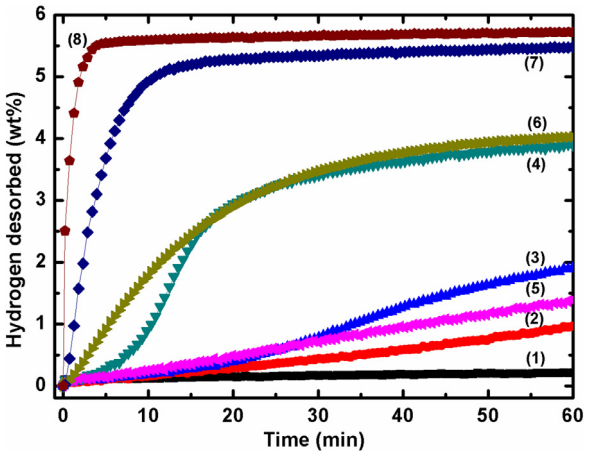

Fig. 4. Isothermal dehydrogenation curves of as-milled MgH_2 and MgH_2 doped with 5 wt% K_2NiF_6 sample at 280 °C (1,5), 300 °C (2,6), 320 °C (3,7) and 340 °C (4,8) and under 1.0 atm hydrogen pressure.

with MgH_2. Thus, further study of the mechanism and catalytic effect has been done on MgH_2 doped 5 wt% K_2NiF_6.

In order to further analyze the dehydrogenation kinetics of the as-milled MgH_2 and MgH_2+5 wt% K_2NiF_6, the dehydrogenation measurements were conducted under 1.0 atm with different temperatures. Fig. 4 compares the isothermal dehydrogenation curves between the un-doped MgH_2 and MgH_2 doped with 5 wt% K_2NiF_6 sample at 280 °C, 300 °C, 320 °C and 340 °C, respectively. The results clearly demonstrated that the MgH_2 doped 5 wt% K_2NiF_6 samples exhibit better hydrogen desorption properties than the un-doped MgH_2. After 60 min dehydrogenation at 280 °C, MgH_2+5 wt% K_2NiF_6 released about 1.4 wt% hydrogen, as shown in Fig. 4. On the other hand, under the same temperature the amount of hydrogen released from the as-milled MgH_2 was only 0.2 wt%. As can be seen in Fig. 4(6–8), it was proven that the dehydrogenation rate for the doped MgH_2 was increased dramatically compared to the un-doped MgH_2. After further heating of the MgH_2 doped 5 wt% K_2NiF_6 samples at 300 °C, 320 °°C and 340 °C over the same period, consequently the samples released hydrogen at about 4.0 wt%, 5.5 wt% and 5.8 wt%, respectively. Meanwhile, as-milled MgH_2 released about 0.9 wt%, 1.9 wt% and 3.9 wt% under the same condition (Fig. 4(2–4)). Thus, the addition of K_2NiF_6 leads to the enhancement of the dehydrogenation kinetics of MgH_2. Such kinetic

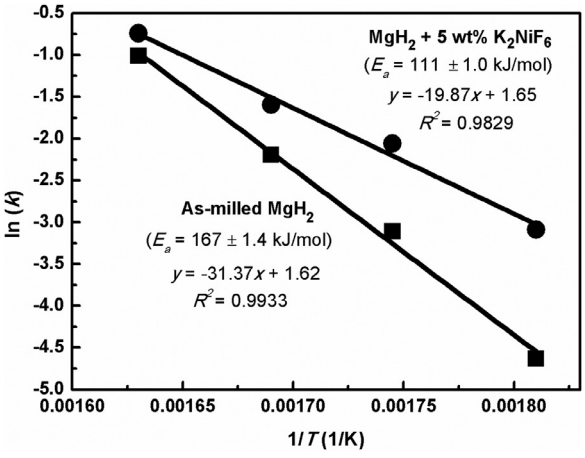

Fig. 5. Arrhenius plots of ln k versus $1/T$ for as-milled MgH_2 and MgH_2 doped with 5 wt% K_2NiF_6.

enhancement is related to the energy barrier for the H_2 to be released from MgH_2.

3.3. Sorption activation energy

The apparent activation energies (E_a) of the as-milled MgH_2 and MgH_2+5 wt% K_2NiF_6 were calculated using the Arrhenius equation as shown in the following:

$$k = k_0 \exp(-E_a/RT) \quad (1)$$

where, k is the rate of dehydrogenation, k_0 is a temperature independent coefficient, E_a is the apparent activation energy for hydride decomposition, R is the gas constant, and T is the absolute temperature. The apparent activation energy, E_a, for hydrogen to be released from the un-doped MgH_2 and 5 wt% K_2NiF_6 doped MgH_2 was explored by plotting the graph of ln k versus $1/T$, as shown in Fig. 5. From the calculations, the apparent activation energy, E_a, for the decomposition of as-milled MgH_2 was 167.0 ± 1.4 kJ/mol. On the other hand, the activation energy was lowered to 111.0 ± 1.0 kJ/mol after doping with K_2NiF_6, which shows a great enhancement in kinetics by 56.0 kJ/mol. Based on the results obtained, it is clearly shown that there are the existence of the synergistic catalysis between MgH_2 and K_2NiF_6. These results are also comparable with the previous studies [45], in which they showed the reduction in activation energy for dehydrogenation of the MgH_2 that was reduced by ball milling and doping with the catalyst. As the activation of MgH_2 was diminished, the dehydrogenation behavior of MgH_2 was also remarkably enhanced.

3.4. Sorption cycling

In the meantime, the investigation of the cycling performance of MgH_2+5 wt% K_2NiF_6 was also carried out. Fig. 6 presents the isothermal rehydrogenation kinetics of the MgH_2 doped 5 wt% K_2NiF_6 that performed at a temperature of 320 °C and under a pressure of 33.0 atm of H_2. The cycle life studies of the composite have been investigated across ten cycles. These result shows that there are some degradation after prolonged time. However, the values of the degradation were too small. The absorption kinetics shows good hydrogen absorption properties even after completing the 10th cycle, with a hydrogen capacity of about 5.1 wt% within 60 min. In addition, Fig. 7 shows the isothermal dehydrogenation kinetics of the same samples that presents the life cycle of desorption kinetics. It can be seen that the hydrogen desorption showed some declination after prolonged cyclic with just involving

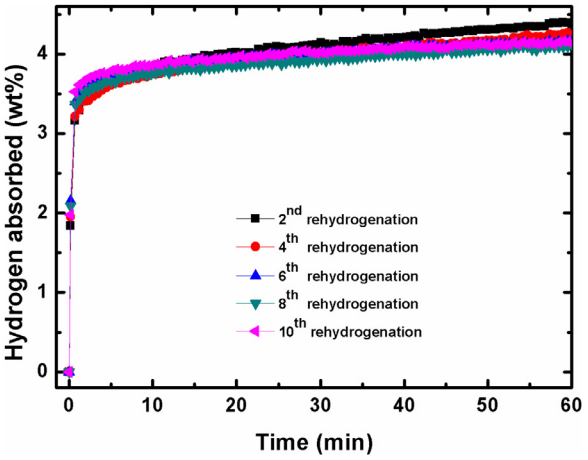

Fig. 6. Isothermal rehydrogenation kinetics of the MgH_2+5 wt% K_2NiF_6 composite in the 2nd, 4th, 6th, 8th and 10th cycles at 320 °C and under 33.0 atm hydrogen pressure.

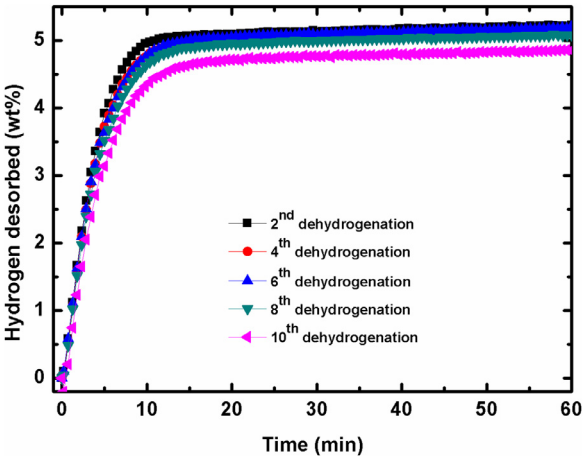

Fig. 7. Isothermal dehydrogenation kinetics of the MgH_2+5 wt% K_2NiF_6 composite in the 2nd, 4th, 6th, 8th and 10th cycles at 320 °C and under 33.0 atm hydrogen pressure.

small amount of hydrogen. The hydrogen desorption continued to be good within 60 min after completing the ten cycles with a capacity of about 4.9 wt%. All the results show that K_2NiF_6 is a good additive compound for the cycle life of MgH_2.

3.5. Differential scanning calorimetry

The thermal properties of the as-milled MgH_2 and the K_2NiF_6-doped MgH_2 samples were further investigated by DSC, as shown in Fig. 8. Clearly, the curve for the as-milled MgH_2 shows only one strong endothermic process peak at 448.0 °C, which corresponds to the decomposition of the MgH_2. In addition, the DSC curves for the MgH_2+5 wt% K_2NiF_6 sample are similar to those of the as-milled MgH_2 sample, displaying only one endothermic peak at 370.0 °C, which corresponded to the decomposition of the MgH_2 but with the peaks having moved to lower temperatures. The reaction formation enthalpy during the dehydrogenation process can be achieved from the integrated peak areas of DSC curve. From Fig. 8, the reaction formation enthalpy for MgH_2+5 wt% K_2NiF_6 sample is calculated to be 70.4 kJ/mol, which is lower than the values of as-milled MgH_2 (75.5 kJ/mol). This result indicates that the presence of K_2NiF_6 destabilizes MgH_2. It is believed that the reaction between Mg and Ni may play a real role in improving the

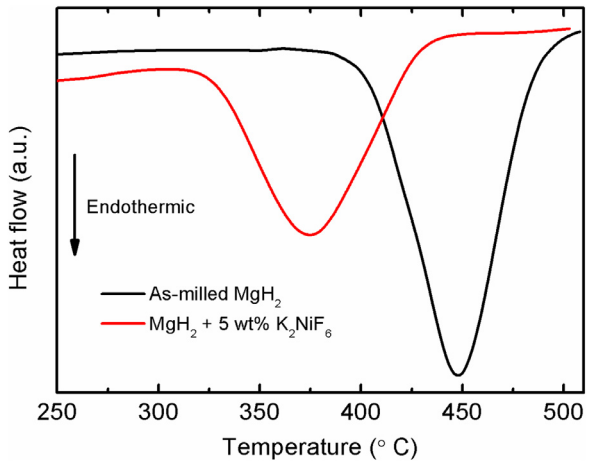

Fig. 8. DSC traces of the as-milled MgH_2 and MgH_2+10 wt% K_2NiF_6 (heating rate: 20 °C/min; argon flow: 30 mL/min).

thermodynamics properties of MgH_2, which was also reported in the literature [27,46].

3.6. Scanning electron microscopy

Fig. 9 presents the SEM images of the as-received MgH_2, as-milled MgH_2 and MgH_2+5 wt% K_2NiF_6. From the results, we can see clearly that the particle size of a sample before undergoing the process of ball milling is larger than the milled sample. As shown in Fig. 9(a), the particle size of as-received MgH_2 sample was larger than 100 μm and angular in shape. Meanwhile, Fig. 9(b) shows the sample of MgH_2 that has encountered the ball milling process for 1 h and exhibits the average size of the MgH_2 particles to be decreased dramatically. Moreover, the particle size was not homogenous with some agglomeration, which was identified in the sample. Fig. 9(c) revealed that MgH_2 doped with 5 wt% K_2NiF_6 had the smallest particle size compared to the as-received and as-milled MgH_2. The smallest size of particle was increasing the surface area of contact to the MgH_2, which can lead to the increasing of rate of reaction for MgH_2.

3.7. X-ray diffraction

To further explore the reaction progress and mechanism of the composites, XRD measurements were performed on the MgH_2+5 wt% K_2NiF_6. The XRD patterns for MgH_2+5 wt% K_2NiF_6 after 1 h of ball milling, after dehydrogenation at 450 °C and after rehydrogenation process at 320 °C and under 33.0 atm hydrogen pressure, are shown in Fig. 10. From Fig. 10(1), it was clearly illustrated that only single MgH_2 peak was detected in the milled sample. The fact that no K_2NiF_6-contained phase detection might be due to the little amount of K_2NiF_6 detected in the XRD machine. Apart from that, after the ball milling, the peaks of K_2NiF_6 might be transformed into an amorphous state. In the dehydrogenation process at 450 °C spectra, as shown in Fig. 10(2), the MgH_2 from the as-milled pattern was fully transformed to Mg. This process showed that the dehydrogenation of MgH_2 was completed. The conversion of the MgH_2 to Mg is shown in the following equation:

$$MgH_2 \rightarrow Mg + H_2 \quad (2)$$

Furthermore, slight peak of KF, KH, and Mg_2Ni appeared after the dehydrogenation process, suggesting that the KF, KH, and Mg_2Ni elements are active species in the combinations of MgH_2 with the K_2NiF_6. The creation of Mg_2Ni element may arise from

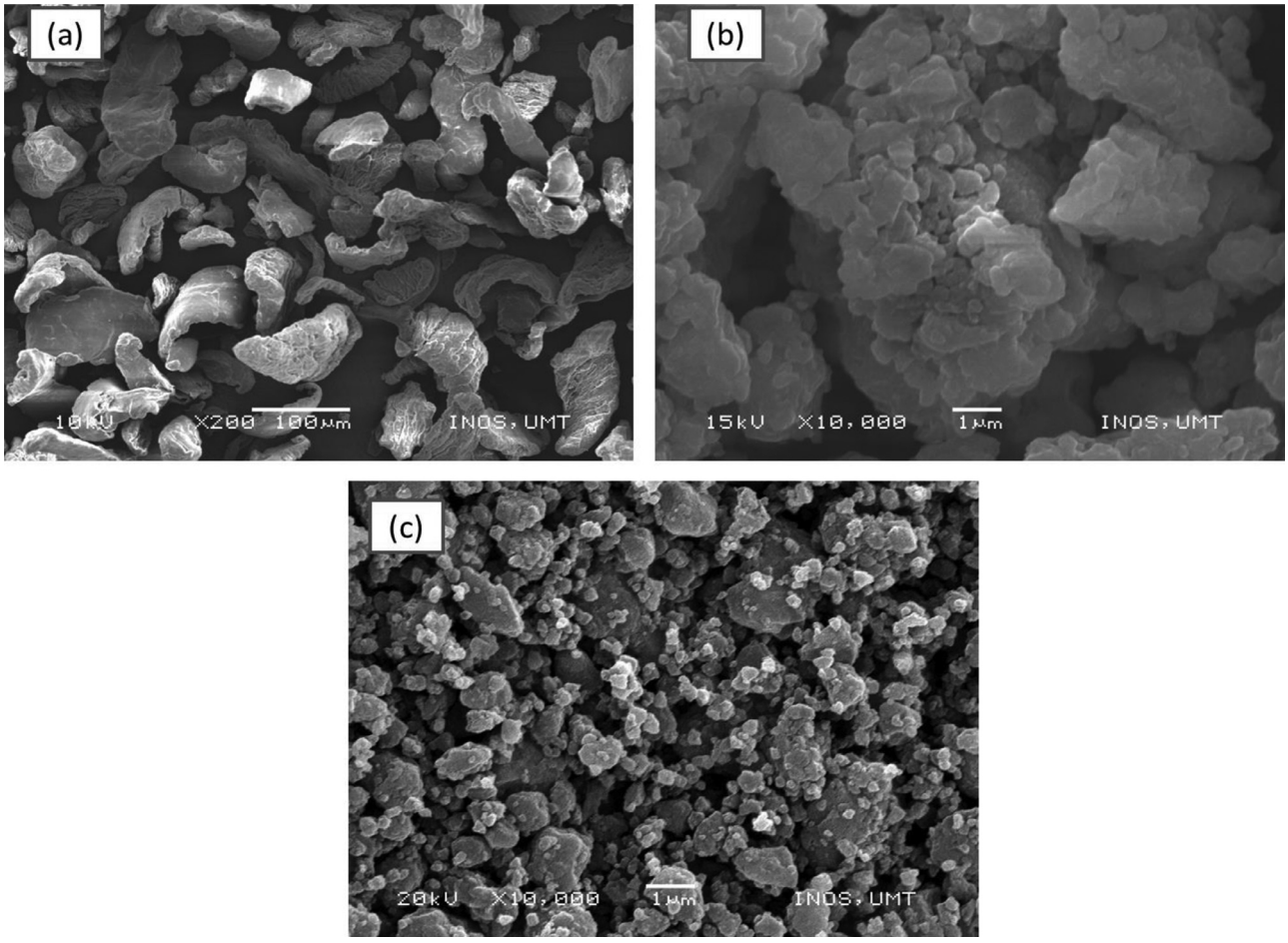

Fig. 9. The SEM images of the (a) as-received MgH_2, (b) as-milled MgH_2 and (c) MgH_2 + 5 wt% K_2NiF_6.

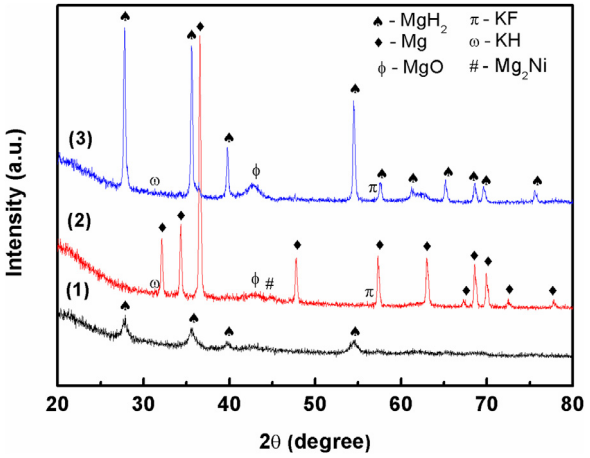

Fig. 10. XRD patterns of the MgH_2 + 5 wt% K_2NiF_6 (1) after 1 h ball milling, (2) after dehydrogenation at 450 °C and (3) after rehydrogenation at 320 °C.

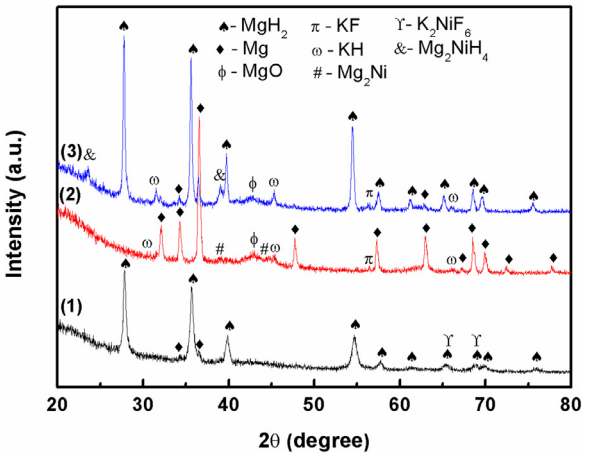

Fig. 11. XRD patterns of the MgH_2 + 20 wt% K_2NiF_6 (1) after 1 h of milling, (2) after dehydrogenation at 450 °C and (3) after rehydrogenation at 320 °C.

the reaction of Mg and Ni that occurred during the heating process. A small amount of MgO is also detected in the peak that resulted from the little oxygen contamination. The patterns in the Fig. 10(3) present the results for the re-dehydrogenation of MgH_2 doped 5 wt% K_2NiF_6 at 320 °C. The results showed that the Mg phase was largely transformed into MgH_2. The peak of KF and KH remained unchanged with a small amount of MgO.

Since only slight peaks of KF, KH, and Mg_2Ni are detected in the phase composition of the sample with 5 wt% K_2NiF_6 by XRD, the sample of MgH_2 with 20 wt% K_2NiF_6 was prepared in order to study the details of the phase structure. Fig. 11 shows the XRD patterns of the MgH_2 doped 20 wt% K_2NiF_6 after 1 h of milling, after dehydrogenation at 450 °C, and after rehydrogenation at 320 °C under hydrogen pressure of 33.0 atm.

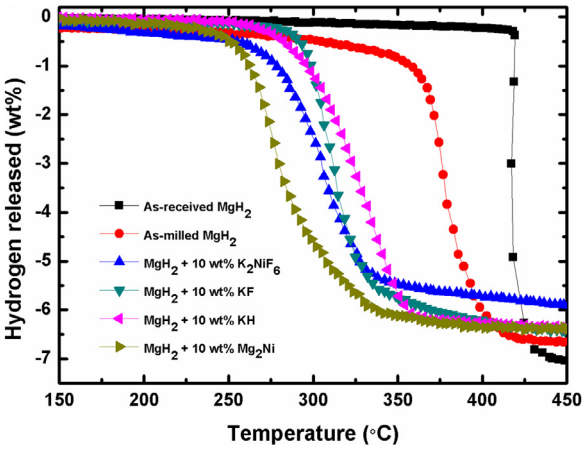

Fig. 12. TPD patterns for the dehydrogenation of the as-received MgH_2, as-milled MgH_2 and the MgH_2 doped with 10 wt% K_2NiF_6, KF, KH and Mg_2Ni.

After 1 h of ball milling technique, MgH_2 phase was detected together with some peaks of Mg and K_2NiF_6, as illustrated in the Fig. 11(1). The appearance of some peaks of Mg shows that during the ball milling process, the hydrogen will be released by MgH_2. This result is correlated with the result obtained in the PCT experiment. On the other hand, after increasing the amount of K_2NiF_6 to 20 wt%, the peaks of the catalyst appeared and showed that the amount was largely enough to be detectable by the XRD machine compared to the 5 wt% K_2NiF_6. After dehydrogenation at 450 °C, as shown in Fig. 11(2), there are additional diffraction peaks of KH and Mg_2Ni along with peaks of KF and MgO that are still visible compared to 5 wt% K_2NiF_6. The results after dehydrogenation at 450 °C showed that the MgH_2 has fully transformed to Mg. Meanwhile, in the Fig. 11(3), it was clearly seen that Mg has largely transformed to MgH_2 for rehydrogenated sample, but there were still little peaks of Mg. Such phenomena might occur due to the Mg not being fully reversible in that stage. The peaks of KF and KH remained unchanged after rehydrogenation, along with the peak of MgO due to the slight oxygen contamination. The peaks of Mg_2NiH_4 were also detected in the pattern due to the Mg_2Ni elements absorbing hydrogen during the rehydrogenation process as follow:

$$Mg_2Ni + 2H_2 \rightarrow Mg_2NiH_4 \quad (3)$$

XRD examination of the dehydrogenated K_2NiF_6-doped MgH_2 samples identified the formation of KF, KH, and Mg_2Ni. The formation of KF, KH and Mg_2Ni encouraged us to speculate that KF, KH and Mg_2Ni may have been acting as a real catalyst. Therefore, in order to verify the effects of KF, KH and Mg_2Ni, the samples of MgH_2 doped with 10 wt% KF, KH and Mg_2Ni were prepared, and the TPD patterns for the dehydrogenation were shown in Fig. 12. It is clearly seen that the onset dehydrogenation temperatures of MgH_2 were improved by doping with KF, KH, and Mg_2Ni comparing to that of the as milled MgH_2. This specified that in-situ generated K, Ni and F species have played an important role and thus the improvement of the dehydrogenation performance of MgH_2–K_2NiF_6 system was more likely to be a synergistic effect. However, the performances of the active species of KF and KH were not as significant as that of the MgH_2 doped with K_2NiF_6. This is may be due to that the samples doped with KF and KH achieved lower dispersion on the MgH_2 surface and less compact phase segregation than the sample doped with K_2NiF_6, resulting from the reaction of MgH_2 with K_2NiF_6 during the heating process which subsequently precipitated KF and KH particles. For the sample doped with Mg_2Ni, it appears that Mg_2Ni is a more effective catalyst than K_2NiF_6. Sabitu et al. [47] demonstrated that doping MgH_2 with Mg_2Ni reduced the onset decomposition temperature. The reaction between MgH_2 and Mg_2Ni during dehydrogenation process that formed the Ni particle may play an important role in the improvement of MgH_2 storage properties. In addition, as discussed in the literatures, Ni is well-known as one the effective catalyst in improving the performance of hydrogenation properties of MgH_2.

From the results obtained, the formation of in-situ active species of KF, KH and Mg_2Ni, which resulted from the dehydrogenation process of MgH_2 and K_2NiF_6, may play an important role to improve the sorption properties of MgH_2. The formation of KF may take place due to the interaction of MgH_2 with K_2NiF_6 during the heating process; which shows that the K_2NiF_6 component in the MgH_2–K_2NiF_6 sample plays a catalytic role through the formation of F-containing catalytic elements. Many studies have reported that the active function of the F anion is important to improve the hydrogen sorption properties of MgH_2 [20,48]. The fluorine based product, KF, may contribute to the enhancement of the de/rehydrogenation kinetics by serving as the active site for nucleation and creation of the dehydrogenated product by shortening the diffusion distance of the reaction ions.

In addition, previous studies [49,50] had reported that the improvement of the hydrogen storage properties in the MgH_2/K_2TiF_6 and MgH_2/K_2ZrF_6 system is related to the combinations of the catalytic effects of KH/TiH_2 and KH/ZrH_2. It is because KH, TiH_2, and ZrH_2 particles precipitated during the heating process might achieve higher dispersion on the MgH_2 surface and higher compact phase segregation than the as-milled composite. Thus, the species will generate a synergetic effect and improve the hydrogen storage properties of MgH_2. In addition, previous studies had shown that the addition of KH can significantly improve the dehydrogenation properties of $NaAlH_4$ and $Mg(NH_2)_2/2LiH$ systems [40,41,51]. In the meantime, a study by Mao et al. [3] suggested that Mg_2Ni, $MgCl_2$ and Mg_2Co act as a real catalyst in improving the hydrogen sorption kinetic properties of MgH_2. Furthermore, the study also indicated that the Mg_2Ni is more active than Mg_2Co because the dehydrogenation of MgH_2 doped with $MgCl_2$ and Mg_2Ni is better compared to that doped with the combinations of $MgCl_2$ and Mg_2Co. In addition, Sabitu et al. [47] reported that the kinetics of MgH_2 has been improved after doping with Mg_2Ni and TiH_2, in which Mg_2Ni being more effective. Therefore, from all the results obtained in this study, it can be concluded that the formation of in situ active species may be actually responsible for the catalytic effects, and thus further enhance the hydrogen storage properties of the MgH_2.

4. Conclusions

In summary, we have found a remarkable enhancement in hydrogen storage performances of MgH_2 by introducing K_2NiF_6 as a catalyst. Among the different amounts of K_2NiF_6 added, analysis showed that the $MgH_2 + 5$ wt% K_2NiF_6 was the best composite to enhance the hydrogen storage properties of MgH_2. The $MgH_2 + 5$ wt% K_2NiF_6 sample exhibited the lower onset dehydrogenation temperature at 260 °C, whereby decreasing the desorption temperature by about 95 °C and 157 °C compared to the as-milled and as-received MgH_2, respectively. From the sorption kinetics measurements, the doped composite of 5 wt% had the fastest kinetics rate. A hydrogen absorption capacity of 3.7 wt% was reached after 2 min in the $MgH_2 + 5$ wt% K_2NiF_6, while the as-milled MgH_2 only absorbed 3.0 wt% of hydrogen under the same conditions. On the other hand, for released kinetics, the MgH_2 doped with 5 wt%, K_2NiF_6 released about 4.9 wt% hydrogen in 10 min of dehydrogenation, but almost no hydrogen was released at this temperature from the as-milled MgH_2 sample in the same period. The results from Arrhenius plot showed that the activation energy for the

hydrogen desorption of $MgH_2 + 5$ wt% K_2NiF_6 was reduced by approximately 56.0 kJ/mol compared to the as-milled MgH_2. From the experimental results, it is believed that the formations of the new products of KF, KH and Mg_2Ni that are formed during the heating process worked together as active elements to improve the hydrogen storage properties of MgH_2.

Acknowledgments

The authors would like to express gratitude to Universiti Malaysia Terengganu for providing the facilities to carry out this project. The authors also acknowledge the Ministry of Higher Education Malaysia to financially support this project through the Fundamental Research Grant Scheme (FRGS 59362). N.N. Sulaiman, N. Juahir, N.S. Mustafa, and F.A. Halim Yap are thankful to the Ministry of Higher Education Malaysia for the My Brain15 scholarship.

References

[1] A.F. Dalebrook, W. Gan, M. Grasemann, S. Moret, G. Laurenczy, Chem. Commun. 49 (2013) 8735–8751.
[2] H. Imamura, K. Yoshihara, M. Yoo, I. Kitazawa, Y. Sakata, S. Ooshima, Int. J. Hydrogen Energy. 32 (2007) 4191–4194.
[3] J. Mao, Z. Guo, X. Yu, H. Liu, Z. Wu, J. Ni, Int. J. Hydrogen Energy. 35 (2010) 4569–4575.
[4] J. Huot, G. Liang, S. Boily, A. Van Neste, R. Schulz, J. Alloys Compd. 293-295 (1999) 495–500.
[5] A. Zaluska, L. Zaluski, J.O. Ström-Olsen, J. Alloys Compd. 288 (1999) 217–225.
[6] R.A. Varin, T. Czujko, Z. Wronski, Nanotechnology 17 (2006) 3856.
[7] N. Juahir, N.S. Mustafa, A. Sinin, M. Ismail, RSC Adv 5 (2015) 60983–60989.
[8] L. Zhang, X. Xiao, C. Xu, J. Zheng, X. Fan, J. Shao, S. Li, H. Ge, Q. Wang, L. Chen, J. Phys. Chem. C. 119 (2015) 8554–8562.
[9] M. Ismail, Y. Zhao, X.B. Yu, S.X. Dou, RSC. Adv 1 (2011) 408–414.
[10] H. Liu, X. Wang, Y. Liu, Z. Dong, H. Ge, S. Li, M. Yan, J. Phys. Chem. C. 118 (2014) 37–45.
[11] M. Ismail, Y. Zhao, S.X. Dou, Int. J. Hydrogen Energy. 38 (2013) 1478–1483.
[12] Y. Zhang, Q.-F. Tian, S.-S. Liu, L.-X. Sun, J. Power Sour. 185 (2008) 1514–1518.
[13] M. Ismail, Y. Zhao, X.B. Yu, J.F. Mao, S.X. Dou, Int. J. Hydrogen Energy. 36 (2011) 9045–9050.
[14] G. Liang, J. Huot, S. Boily, A. Van Neste, R. Schulz, J. Alloys Compd. 292 (1999) 247–252.
[15] X.B. Yu, Y.H. Guo, Z.X. Yang, Z.P. Guo, H.K. Liu, S.X. Dou, Scr. Mater. 61 (2009) 469–472.
[16] X.B. Yu, Y.H. Guo, H. Yang, Z. Wu, D.M. Grant, G.S. Walker, J. Phys. Chem. C. 113 (2009) 5324–5328.
[17] X.B. Yu, Z.X. Yang, H.K. Liu, D.M. Grant, G.S. Walker, Int. J. Hydrogen Energy. 35 (2010) 6338–6344.
[18] M. Ismail, Energy 79 (2015) 177–182.
[19] I.E. Malka, T. Czujko, J. Bystrzycki, Int. J. Hydrogen Energy. 35 (2010) 1706–1712.
[20] L.P. Ma, X.D. Kang, H.B. Dai, Y. Liang, Z.Z. Fang, P.J. Wang, P. Wang, H.M. Cheng, Acta Mater 57 (2009) 2250–2258.
[21] M. Ismail, Int. J. Hydrogen Energy. 39 (2014) 2567–2574.
[22] S.-A. Jin, J.-H. Shim, Y.W. Cho, K.-W. Yi, J. Power Sources. 172 (2007) 859–862.
[23] M. Ismail, Y. Zhao, X.B. Yu, S.X. Dou, Energy Edu. Sci. Technol. Part A Energy Sci. Res. 30 (2012) 107–122.
[24] M. Abdellatief, R. Campostrini, M. Leoni, P. Scardi, Int. J. Hydrogen Energy. 38 (2013) 4664–4669.
[25] A. Patah, A. Takasaki, J.S. Szmyd, Int. J. Hydrogen Energy. 34 (2009) 3032–3037.
[26] G. Barkhordarian, T. Klassen, R. Bormann, Scr. Mater. 49 (2003) 213–217.
[27] Q. Wan, P. Li, J. Shan, F. Zhai, Z. Li, X. Qu, J. Phys. Chem. C. 119 (2015) 2925–2934.
[28] A. Ranjbar, M. Ismail, Z.P. Guo, X.B. Yu, H.K. Liu, Int. J. Hydrogen Energy. 35 (2010) 7821–7826.
[29] N. Hanada, T. Ichikawa, H. Fujii, J. Phys. Chem. B. 109 (2005) 7188–7194.
[30] G. Barkhordarian, T. Klassen, R. Bormann, J. Phys. Chem. B. 110 (2006) 11020–11024.
[31] C.X. Shang, M. Bououdina, Y. Song, Z.X. Guo, Int. J. Hydrogen Energy. 29 (2004) 73–80.
[32] J.L. Bobet, E. Akiba, Y. Nakamura, B. Darriet, Int. J. Hydrogen Energy. 25 (2000) 987–996.
[33] C.Z. Wu, X.D. Yao, H. Zhang, Int. J. Hydrogen Energy. 35 (2010) 247–252.
[34] J. Zhang, L.Q. Sun, Y.C. Zhou, P. Peng, Comput. Mater. Sci. 98 (2015) 211–219.
[35] F. Cova, P. Arneodo Larochette, F. Gennari, Int. J. Hydrogen Energy. 37 (2012) 15210–15219.
[36] Y. Luo, P. Wang, L.-P. Ma, H.-M. Cheng, J. Alloys Compd. 453 (2008) 138–142.
[37] L.-P. Ma, P. Wang, H.-M. Cheng, Int. J. Hydrogen Energy. 35 (2010) 3046–3050.
[38] L.-C. Yin, P. Wang, X.-D. Kang, C.-H. Sun, H.-M. Cheng, Phys. Chem. Chem. Phys. 9 (2007) 1499–1502.
[39] S. Deledda, A. Borissova, C. Poinsignon, W.J. Botta, M. Dornheim, T. Klassen, J. Alloys Compd 404–406 (2005) 409–412.
[40] P. Wang, X.D. Kang, H.M. Cheng, J. Appl. Phys. 98 (2005) 5.
[41] J. Wang, T. Liu, G. Wu, W. Li, Y. Liu, C.M. Araújo, R.H. Scheicher, A. Blomqvist, R. Ahuja, Z. Xiong, P. Yang, M. Gao, H. Pan, P. Chen, Angew. Chem. Int. Ed. 48 (2009) 5828–5832.
[42] B.-X. Dong, L. Song, Y.-L. Teng, J. Ge, S.-Y. Zhang, Int. J. Hydrogen Energy. 39 (2014) 13838–13843.
[43] A. Ranjbar, Z.P. Guo, X.B. Yu, D. Wexler, A. Calka, C.J. Kim, H.K. Liu, Mater. Chem. Phys. 114 (2009) 168–172.
[44] C.J. Webb, J. Phys. Chem. Solids. 84 (2015) 96–106.
[45] M. Ismail, N. Juahir, N.S. Mustafa, J. Phys. Chem. C. 118 (2014) 18878–18883.
[46] C. Zhou, Z.Z. Fang, C. Ren, J. Li, J. Lu, J. Phys. Chem. C. 117 (2013) 12973–12980.
[47] S.T. Sabitu, G. Gallo, A.J. Goudy, J. Alloys Compd. 499 (2010) 35–38.
[48] L. Xie, Y. Liu, Y.T. Wang, J. Zheng, X.G. Li, Acta Mater 55 (2007) 4585–4591.
[49] N.S. Mustafa, M. Ismail, Int. J. Hydrogen Energy. 39 (2014) 15563–15569.
[50] F.A. Halim Yap, N.S. Mustafa, M. Ismail, RSC. Adv 5 (2015) 9255–9260.
[51] Y. Liu, C. Liang, H. Zhou, M. Gao, H. Pan, Q. Wang, Chem. Commun. 47 (2011) 1740–1742.